1 **Climate explains recent population divergence, introgression and persistence in tropical**

2 **mountains: phylogenomic evidence from Atlantic Forest warbling finches**

3

4 Fábio Raposo do Amaral[1†*], Diego F. Alvarado-Serrano[2†], Marcos Maldonado-Coelho[1], Katia

5 C. M. Pellegrino[1], Cristina Y. Miyaki[3], Julia A. C. Montesanti[1], Matheus S. Lima-Ribeiro[4],

6 Michael J. Hickerson[2], Gregory Thom[3]

7

8 1 Universidade Federal de São Paulo. Departamento de Ecologia e Biologia Evolutiva. Rua

9 Professor Artur Riedel, 275, Diadema, SP, 09972-270, Brazil.

10 2 Biology Department, City College of New York, New York, NY 10031, USA

11 3 Universidade de São Paulo, Departamento de Genética e Biologia Evolutiva. Rua do Matão,

12 277, Cidade Universitária, São Paulo, SP, 05508-090, Brazil.

13 4 Departamento de Ciências Biológicas, Universidade Federal de Goiás, Campus Jataí, Jataí,

14 GO, Brasil

15 [†] These authors contributed equally to this study

16 * To whom correspondence should be addressed: fabioraposo@gmail.com

17

18 Running title: Isolation and contact in Atlantic Forest mountains

19 Keywords: Atlantic Forest biogeography, cold-adapted birds, demographic history,

20 ultraconserved elements

21

22

23

24

25

26

27

28

29

30

31

32

33

34

Abstract

Taxa with disjunct distributions are common in montane biotas and offer excellent opportunities to investigate historical processes underlying genetic and phenotypic divergence. In this context, subgenomic datasets offer novel opportunities to explore historical demography in detail, which is key to better understand the origins and maintenance of diversity in montane regions. Here we used a large ultraconserved elements dataset to get insights into the main biogeographic processes driving the evolution of the Montane Atlantic Forest biota. Specifically, we studied two species of warbling finches disjunctly distributed across a region of complex geological and environmental history. We found that a scenario of three genetically differentiated populations is best supported by genomic clustering methods. Also, demographic simulations support simultaneous isolation of these populations at ~10 kya, relatively stable population sizes over recent time, and recent gene flow. Our results suggest a dual role of climate: population divergence, mediated by isolation in mountain tops during warm periods, as well as population maintenance - allowing persistence mediated by shifts in elevation distribution during periods of climate change, with episodic bouts contact and gene flow. Additional support for the role of climate comes from evidence of their contact in a recent past. We propose that two major gaps, which we call São Paulo and Caparaó subtropical gaps, have been historically important in the divergence of cold adapted organisms in the Atlantic Forest, and could be associated to cryptic diversity. Finally, our results suggest that shallow divergence and past gene flow may be common in montane organisms, but complex demographic histories may be detectable only when using subgenomic or genomic datasets.

57   **Introduction**
58
59   Montane organisms often exhibit intriguing patterns of disjunct distributions, which are

60   frequently associated to phenotypic divergence. Among the many mechanisms that have been

61   proposed to explain such patterns, the ones with the strongest support are the historical

62   fragmentation of formerly continuous habitats and dispersal (Mayr & Diamond 1976; Patton &

63   Smith 1992; Knowles & Massatti 2017) asssociated with rugged topography and climate

64   fluctuations. That is, changes in climate over time, which are well known to promote shifts in

65   the elevational distributions of suitable habitats and associated organisms (Hooghiemstra &

66   Van der Hammen 2004, Moritz et al. 2008, Chen et al. 2009), could lead to cyclical isolation

67   and connection of population through temporal bridges (Brown 1971, McCormack et al. 2009).

68   During the late Pleistocene glacial periods, warmer periods often lead to isolation in

69   high-elevation habitat pockets, whereas colder periods often lead to range expansion into lower

70   elevations and previously unsuitable regions. Under this scenario, warmer periods (such as the

71   current interglacial) would create opportunities for population divergence by genetic drift and

72   natural selection, while colder periods might promote secondary contact and genetic

73   homogenization of previously isolated populations. This interplay between selection and drift

74   with topography and a dynamic climate could lead not only to genetic divergence, but to the

75   evolution of reproductive isolation, thus rendering mountains as potential hotspots of

76   population divergence and speciation (Fjeldsa 1994, McCormack et al. 2009). Alternatively,

77   isolation could be initially mediated by topographic changes. For example, the splitting of

78   formerly continuous highlands into multiple isolated mountain ranges could be the result of

79   geological changes, and organisms adapted to higher habitats would then become separated by

80   ecologically unsuitable valleys. Under such scenario, population divergence should be

81   temporally associated to geotectonic changes (Badgley 2010).

82   These biogeographic processes likely have played an important role in the building up

83   of the enormous diversity found in mountain regions (Graham et al. 2014, Antonelli 2015;

84   Knowles & Massatti 2016). However, their exact contribution is not well understood. In

85   particular, the evolutionary processes underlying the high levels of biological diversity in the

86   South American Montane Atlantic Forest are yet to be elucidated. The Montane Atlantic Forest

87   (hereafter MAF) is a cradle of biodiversity (Stotz et al. 1996) and has great potential to provide

88   a wealthy natural laboratory for evolutionary research since its high levels of endemism likely

89   encompass a plethora of diversification mechanisms. In particular, MAF organisms showing

90   phenotypic breaks that coincide with major highlands are especially interesting models for

91   montane phylogeography, as such pattern presumably reflects genome-wide divergence
92   resulting from an interplay between climate, topography and the evolutionary outcomes of drift,
93   selection and gene flow. Of these, vagile organisms such as birds may be particularly useful
94   models to understand large-scale historical events, as their fidelity to specific habitats and high
95   dispersal ability may promote genetic differentiation and homogenization, except in face of
96   strong events of habitat isolation.

97   Much of what is known about the Atlantic Forest comes from studies of either lowland
98   species or species with broad elevational distributions (e.g. Cabanne et al. 2007, Carnaval et al.
99   2009. Maldonado-Coelho 2012, Amaral et al. 2013, Carnaval et al. 2014), and less than a
100   handful of phylogeographic studies have investigated cold-adapted species whose distributions
101   include mostly montane habitats (e.g. Amaro et al. 2013, Batalha-Filho et al. 2012, Peres et al.
102   2015, Frikowski et al. 2016, Françoso et al. 2016, Pie et al. 2018). Conclusions from the few
103   studies on MAF-inhabiting species are often discordant; consequently, there is still little
104   consensus about what are the major drivers of diversification in the MAF. A common finding
105   by many of them is the lack of both population structure and strong demographic fluctuations,
106   which could speak against Pleistocene climatic fluctuations as major drivers of population
107   divergence and diversification in MAF organisms. Importantly, all but one (Pie et al. 2018) of
108   the studies performed so far were based on five or less loci, raising the possibility that shallow
109   population structure—which is expected under recent climate fluctuations—may have been
110   overlooked (Amaral et al. 2018). Furthermore, none of these studies have performed
111   demographic analyses explicitly testing for historical gene flow among currently isolated and
112   genetically structured populations—a prediction of montane climate-driven dynamics.

113   Here we use the largest population-level sub-genomic dataset of any MAF organism
114   and coalescent-based methods to ask (1) how does genetic variation relates to distribution
115   breaks in the MAF, and (2) what are the influences of climate and topographic evolution (i.e.
116   mountain building) on the current patterns of genetic variation in endemic Atlantic Forest
117   montane birds. To address these questions we use two common cold-adapted species of
118   Atlantic Forest warbling finches as models: the Gray-Throated Warbling Finch (*Microspingus
119   cabanisi*) and the Buff-Throated Warbling Finch (*Microspingus lateralis*). Their distributions
120   and phenotypic breaks are congruent with major isolated highlands in S and SE Brazil (Assis et
121   al. 2007), and a detailed phylogeographic analysis of these species represents a fundamental
122   step towards a better understanding of population history in MAF and biotic diversification in
123   tropical montane systems as a whole.

124 **Methods**

125

126 *Study system: biological models and geological and environmental history of the MAF*

127   The two warbling finches studied here are sister-species (Amaral *et al.* 2015), once

128 considered conspecific (Assis et al. 2007), and whose combined distributions cover most of the

129 MAF. The northern species, *M. lateralis* inhabits highland areas above 900 m of two major

130 isolated mountain ranges in SE Brazil, the Mantiqueira and the northern portion of the Serra do

131 Mar. This species also occurs in the Caparaó highlands, an isolated northernmost massif of the

132 Mantiqueira mountain range (Fig.1). The southern species, *M. cabanisi*, occurs in the southern

133 portion of Serra do Mar and also in the Serra Geral mountain range mostly above 900 m, but

134 also in lower elevation areas towards its southern limit, which includes areas in Argentina and

135 Paraguay (Assis et al. 2007). These two species are currently separated by more than 100 km of

136 lower elevation forest habitats (Fig. 1). They differ phenotypically in both plumage and

137 vocalizations. Plumage differences are mostly in ventral color (yellow in *M. lateralis* and gray

138 in *M. cabanisi*) and amount of white in tail feathers (more extensive in *M. cabanisi*), whereas

139 the songs and the calls of these species differ in syntax and harmonic structure, respectively

140 (Assis et al 2007).

141   The tectonic processes that originated the eastern Brazilian highlands as well as their

142 ages are still a matter of debate. In one hand, the major uplift events were suggested to have

143 started during the lower Cretaceous (ca. 120 mya) as a consequence of the Gondwanaland

144 breakup (Melo et al. 1985, Franco-Magalhães et al. 2014). On the other hand, the uplift is

145 proposed to have resulted from the three main pulses of Andean orogeny, with the early ages of

146 the mountain ranges (i.e. Serra do Mar) estimated to be ca. 90 mya (Meisling et al. 2001, Karl

147 et al. 2013). Regardless, a range of evidence indicates subsequent multi-episodic uplift events

148 during the upper Cretaceous, the Tertiary and the Quaternary (Freitas 1951, Melo et al. 1985,

149 Almeida & Carneiro 1998, Modenesi-Gauttieri et al. 2002, Tello Saens et al. 2003,

150 Hackspacher et al. 2004, Franco-Magalhães et al. 2014), with the uplift of the Serra do Mar

151 mountain range thought to have extended until recent times (i.e. Holocene, Cogné et al. 2012).

152   Available evidence from fossil pollen records in southern and southeastern Brazil

153 highland sampling sites (> 900 m a.s.l.) at Mantiqueira, Serra do Mar and Serra Geral mountain

154 ranges suggest broadly concordant cold and dry conditions during the last glacial maximum,

155 with forests completely absent or likely present only along ravines and/or at lower altitudes

156 (Behling 1997, 2007, Behling & Pillar 2007, Behling et al. 2007, Oliveira et al. 2008, Ledru et

157 al. 2009, Behling & Safford 2010, Oliveira et al. 2012). The onset of a moister climate after this

158   period favored the return of montane forest species (Behling 1997, Behling & Pillar 2007,

159   Behling et al. 2007, Ledru et al. 2009, Behling and Safford 2010, Oliveira et al. 2012).

160   Importantly, the highland vegetation seems to have had a complex dynamics during the last

161   130,000 yr BP (i.e. late Pleistocene and Holocene), with multiple shifts in community

162   composition and elevational distribution of montane forest plant species (Ledru et al. 2009,

163   Behling & Safford 2010, Oliveira et al. 2012).

164

165   *Sampling and laboratory methods*

166   We sampled 90 individuals (50 of *M. cabanisi* and 40 of *M. lateralis*) in nine

167   localities—10 per locality, spread throughout the species' known distributions (Fig. 1,

168   Supplementary Information Table S1). Specimens were attracted by playback and collected as

169   described in Amaral *et al.* 2012 (see Acknowledgments for permit number and Table S1 for

170   specimen and tissue collection holdings).

171   We extracted total DNA from pectoral muscle using the Qiagen DNeasy kit (Valencia,

172   CA) according to the manufacturer's protocol, including a RNAse treatment. We obtained

173   genomic data using sequence capture and Illumina sequencing of ultraconserved elements

174   (UCEs) using standard protocols (Fairlocth *et al.* 2012) with a few modifications: enrichment

175   was done using 650 probes, targeting 634 loci covering all *Gallus gallus* chromosomes; use of

176   100 bp paired-end Illumina Hiseq 2000 sequencing run, and use of 16 cycles in both pre- and

177   post-capture PCR reactions. Sequencing was performed in two lanes. Library preparation was

178   performed by RAPiD Genomics (Gainesville, FL, USA).

179

180   *Sequence quality control, mtDNA, UCE assembly and SNP calling*

181   We sorted raw sequences by individual tags using Illumina's Casava software. Initial

182   quality control was performed using FastQC 0.10.1 (Andrews 2014). Adapters, barcodes and

183   low quality regions were trimmed using Illumiprocessor 2.0.7 (Faircloth 2014), which

184   processes Illumina sequences using Trimmomatic 0.32.1 (Bolger *et al.* 2014). Assembly,

185   removal of non-UCE loci and final loci aligment was performed with Phyluce 1.4 (Faircloth

186   2014). The largest contig of each locus was used as a reference for mapping individual reads

187   using BWA-mem (Li 2013) and SNP calling, which was performed using GATK (McKenna *et*

188   *al.* 2010). We kept only >Q30 SNPs for downstream analyses. We sampled one random SNP

189   per locus from the collection of all zero-missing biallelic SNPs recovered for the locus. We

190   removed Z-linked SNPs using a local BLAST search based on the zebra-finch Z chromossome

191   (Emsembl taeGut3.2.4) to avoid any bias due to the idiosincratic evolution of sex

192   chromossomes and different ploidy (unfortunately the limited number of Z-linked SNPs

193   recovered precluded us from running independent analyses on this dataset). Since mtDNA is a

194   common subproduct of sequence capture experiments (see Amaral *et al.* 2015), we also

195   isolated complete cythochrome b sequences from assemblies that were generated by Phyluce

196   using a local BLAST search based on the complete mitogenome of *Microspingus lateralis*

197   (Genbank NC_028039.1) to obtain a Median Joining Network using POPART v 1.7 (Leigh &

198   Bryant 2015).

199

200   *Population structure*

201   We explored population structure first with sparse non-negative matrix factorization

202   (sNMF, Frichot et al. 2014, implemented in the R package LEA, Frichot & Olivier 2015) as

203   well as with the multivariate Discriminant Analysis of Principal Components (Jombart *et al.*

204   2010). The sNMF runs were performed for a range of K values from 1 to 9 (following the

205   number of localities), with 500 runs per K. We used the minimum cross-entropy method to

206   identify the best fitting K. Runs with the lowest values of minimum entropy were selected.

207   Since sNMF's regularization parameter alpha may affect the inferences (Frichot et al. 2014),

208   we evaluated the results under different values of alpha (1, 10, 100 and 1,000). To further

209   assess population structure we ran a DAPC analysis using a k-clustering algorithm to

210   determine the *a priori* grouping of individuals based on the Bayesian Information Criterion

211   (BIC). The first set of principal components accounting for 80% of the variance was included

212   in the analyses.

213

214   *Inference of historical processes*

215   Based on the results from the previous analyses (Fig. 2), we tested 12 alternative

216   models to assess the most likely diversification scenario for *Microspingus*. The models tested

217   explored the relationship of the three genetic clusters inferred by sNMF, the presence of gene

218   flow and instantaneous population size change after divergence (Fig. 3). To compare simulated

219   data under each specific demographic model with the empirical data we implemented a

220   coalescent model-based approach using Fastsimcoal2 (FSC; Excoffier et al. 2013). Since FSC

221   summarizes the complexity of the data by using the site frequency spectrum (SFS) as summary

222   statistics, we first estimated the empirical multi-SFS (single SFS with all populations included)

223   in $\partial a \partial i$ 1.7 (Gutenkunst et al. 2009). For each demographic model we ran 50 independent

224   replicates, retaining the parameters that maximized the composite likelihood across all

225   iterations. Parameter optimization was performed through 50 cycles of the Brent algorithm and

226   the composite likelihood calculated using 100,000 simulations per replicate. The runs with the

227   highest likelihood of each model were used in model selection using Akaike Information

228   Criterion (AIC; Akaike 1973), AIC=2k-2ln(L), where k is the number of parameters estimated

229   in the model and L the composite likelihood value. The model with best fit had its confidence

230   intervals estimated with 50 parametric bootstrap runs, by simulating multi-SFSs under the

231   maximum likelihood estimates and re-estimating parameters for each of these simulated data

232   sets. For all simulations, we used a rate of 2.5×10^{-9} substitution per site per generation

233   (average of all avian species analysed in Nadachowska-Brzyska et al. 2015) and assumed a

234   generation time of 2.33 years (Maldonado-Coelho 2012).

235

236   **Results**

237
238   *Sequencing results*

239   We obtained 634 UCE loci with median length of 633 bp (range: 216-811 bp) and 8,465

240   SNPs passed our quality filtering. Each UCE locus had a median of 13 SNPs (range: 1-35). The

241   final dataset containing 1 randomly sampled SNP per variable locus had 588 SNPs.

242   *Population structure*

243   sNMF runs indicated three groups based on the best cross-entropy values across alpha

244   values, with the only exception of alpha of 1,000 showing a smaller cross-entropy value for a

245   single group (Supporting Information Figure S1). Plots based on alpha of 1, 10 and 100 for

246   K=3 support the Caparaó population of *M. lateralis*, the remaining *M. lateralis* populations,

247   and *M. cabanisi* as three distinct clusters with somewhat varying levels of ancestry coefficients

248   (Fig. 2). DAPC based on k-clustering algoritm suggests two as the best number of groups,

249   altough BIC values are very similar among K=1, K=2 and K=3 (246.7343, 246.5362 and

250   247.0419, respectively, Supporting Information Figure S2). These two clusters correspond to:

251   1) the Caparaó population of *M. lateralis* + some *M. cabanisi* individuals and 2) remainig *M.*

252   *lateralis* individuals + remaining *M. cabanisi* individuals (Supporting Information Figure S2).

253   If the three sNMF populations are considered in the DAPC analysis, the groupings are similar:

254   one of them included only *M. lateralis* Caparaó individuals and the other two mostly matched

255   *M. cabanisi* and *M. lateralis* excluding Caparaó (Fig. 2 and Supporting Information Fig. S1).

256   Accordingly, the mtDNA haplotype network showed no haplotypes shared among populations,

257   although some haplotypes of *M. lateralis* were more closely related to those of *M. cabanisi*

258   than to conspecific haplotypes, while Caparaó haplotypes formed a cluster (Fig. 2).

259

260 *Demographic relationships and population history*

261   The best demographic model according to AIC assumed a polytomy of the three

262 populations, presence of assymetric gene flow and stable population sizes after the divergence

263 (Fig. 3; Tables 1 and 2). The second and third best-fit models included alternative branching

264 (instead of simultaneous divergence) with gene flow, but neither supported population size

265 changes (Table 1). Parameter estimations based on the best-fit model supported current

266 effective population sizes (Ne) that were positively related with the modern range size of the

267 three lineages. The geographically most restricted population (i.e. Caparaó) had the smallest

268 Ne, with ~4,000 individuals, followed by the populations with intermediate (rest of *M. lateralis*)

269 and largest (*M. cabanisi*) geographic ranges, with respectively ~11,000 and ~19,500

270 individuals (Table 2). The divergence time estimate supports a very recent (Late Pleistocene)

271 event for the simultaneous separation of the three populations at approximately 12,400 years

272 ago (5,325 generations, Table 2).

273   The estimated gene flow between *M. cabanisi* and *M. lateralis* (excluding Caparaó)

274 was greater (3.15 and 2.65 individuals per generation from *M. lateralis* to *M. cabanisi* and from

275 *M. cabanisi* to *M. lateralis*, respectively) than between *M. lateralis* and the Caparaó population

276 of this species (0.324 and 1.147 individuals per generation from *M. lateralis* to Caparaó and

277 from Caparaó to *M. lateralis*, respectively), potentially reflecting the more isolated and

278 restricted distribution of the Caparaó population (Table 2).

279

280 **Discussion**

281

282 *The dual role of AF mountains: population divergence and persistence*

283

284   Mountains may function both as generators and maintainers of diversity (Fjeldsa et al.

285 2012), and here we show a Atlantic Forest organisms that support this idea. First, the ancient

286 AF highlands may generate diversity by fostering population isolation and divergence, as

287 indicated by our population structure estimates with three distinct groups associated with three

288 isolated mountain ranges. While geotectonic changes could explain phylogeographic breaks in

289 the AF (e.g. Thomé et al. 2010, Amaro et al. 2012, Amaral et al. 2013), the shallow divergences

290 found here cannot be reconciled with the major uplift events of eastern Brazil highlands, which

291 very likely took place long before the estimated recent divergence times (< 20 k years). In

292 addition, support for a model of synchronous isolation among the three populations is

293 especially compelling in terms of large scale effects of climate across the entire range of

294 subtropical AF. Interestingly, the strong population structure found here contradicts previous

295 studies on other co-distributed montane organisms, which did not recover recent (< 100 k years)

296 phylogeographic breaks (Amaro et al. 2012, Batalha-Filho et al. 2012, Peres et al. 2015). These

297 findings suggest that although warbling-finches are forest-associated species that often use

298 forest edges, such ecological flexibility was presumably not sufficient to preclude isolation and

299 divergence. In contrast, the White-browed Warbler (*Myiothlypis leucoblephara*), for example,

300 which is sympatric - and often syntopic - to *M. cabanisi* and *M. lateralis*, did not show

301 detectable population structure (Batalha-Filho et al. 2012). These phylogeographic differences

302 may be due to the interaction of traits and historical processes (see Zamudio et al. 2016 for a

303 review), differences in altitudinal distribution, lack of power of Sanger datasets to detect

304 shallow divergences (Amaral et al. 2018) or a combination of those factors, and warrants

305 additional studies on both novel and previously studied organisms using subgenomic or

306 genomic datasets.

307 Second, it has been long suggested that the MAF (Brown & Ab'Saber, 1979; Brown,

308 1987) and other Neotropical mountains (Fjeldså et al. 1999; García-Moreno & Fjeldså, 2000,

309 Mastretta-Yanes et al. 2018) are safe harbors (i.e refuges) for montane and non-montane

310 organisms during historical periods of harsh climates. Mountains may buffer population size

311 changes of montane forest organisms during historical periods of unsuitable climate by holding

312 moisture in the leeward slopes (Brown & Ab'Saber 1979) and by allowing shifts in elevational

313 distributions, a process that may be even seen in ecological time (Moritz et al. 2008). In line

314 with this observation, our estimates of historical demography echo the lack of strong

315 population size fluctuations found in other co-distributed organisms (Amaro et al. 2012,

316 Batalha-Filho et al. 2012, Peres et al. 2015, Pie et al. 2018), what underscores the notion that

317 montane habitats are important refuges, hampering extinction of isolated population during

318 periods of climate change.

319 While our results illustrate how montane habitats may act both as drivers and keepers of

320 diversity, partial concordance with previous studies, specially in terms of population structure,

321 is intriguing. New comparative phylogenomic studies will help understand the generality of the

322 patterns found here, and contribute to tease apart the effects of history, ecology and issues

323 related to number of loci. We hypothesize that population structure among highland species in

324 the AF will be more common than previously thought, and in many cases may be detectable

325 only using sufficiently sized nuclear datasets (e.g. Pie et al. 2018; present study). Fine-scale

326 inferences of population structure will be essential not only to better describe patterns and infer

327 processes involved in Neotropical montane diversification, but may also reveal important

328 hotspots of divergence and cryptic diversity of conservation importance, which may have been

329 overlooked due to recent divergences (as in the Araripe Highlands, Amaral et al. 2018).

330

331 *Historical climate changes explain diversification in MAF warbling-finches*

332 A main question in the MAF system is whether one can disentangle the relative

333 influence of topography and climate when explaining diversification patterns. For example,

334 under a strict geomorphological model of diversification, genetic divergences among warbling

335 finch populations should be coincident with the known major pulses of uplift of eastern

336 Brazilian highlands during the last ca.100 mya (e.g. Melo et al. 1985, Meisling et al. 2001,

337 Franco-Magalhães et al. 2014). However, we argue that one cannot rule out biogeographic

338 scenarios in which historical climate changes taking place during or subsequent to the major

339 uplift events had a main role on biotic diversification. In fact, the interplay between topography

340 and climate implies that the expected model of diversification for warbling finches and other

341 MAF organisms would be one of isolation and divergence on distinct highlands during the

342 warm-interglacial periods, when populations retracted upwards over the mountains. In addition,

343 any event of genetic admixture (i.e. introgression) between resulting lineages ensued when

344 populations expanded downwards, during cold-glacial periods. The results of our coalescent

345 analyses and the current altitudinal distribution of warbling finches confirm key components of

346 this model. Specifically, the recent estimates of genetic divergence and past admixture (i.e. for

347 the late Pleistocene) as well as their ocurrence on highlands during the present-day

348 warm-interglacial period undoubtedly implicate a strong influence of historical climate

349 changes on range shifts and associated population evolutionary dynamics across a

350 longstanding rugged landscape. One especially intriguing result is the lack of recent variation

351 in effective size despite signs of introgression. We hypothetize that secondary contact may not

352 necessarily involve large population size fluctuation, as shifts in elevational distribution could

353 occur without significant changes in effective size. In addition, small elevational shifts (e.g.

354 only 100 m) could readly connect the two species (Fig. 1). Alternatively, we can also speculate

355 that past gene flow may have erased signs of population expansion and contraction, or limited

356 expansion associated with long-distance dispersal could explain introgression without large Ne

357 variation.

358

359 *Elevational distribution and its role in population isolation*

360 Population structure was detected in the northern species (*M. lateralis*) but was absent

361 in the southern species (*M. cabanisi*), and it is possible that the phylogeographic structure of

362   *Microspingus* warblers may reflect historical differences in forest dynamics between

363   southeastern and southern AF. One interesting biological difference between *M. cabanisi* and

364   *M. lateralis* is their distinct elevational range: populations of *M. lateralis* are found only above

365   900 m, while in the southernmost part of its range, *M. cabanisi* reaches sea-level. This pattern

366   may be a consequence of either thermal niche divergence (Janzen 1967), biological

367   interactions (i.e. competition) or simply a latitudinal compensation of elevational distribution

368   (Barry 1992). In any case, differences in altitudinal ranges across a latitudinal gradient may

369   lead to greater opportunities for isolation in the populations in the northern extreme edges of

370   SE/S subtropical habitats than those in the southern edges. Additional multi-taxon studies are

371   warranted to test this hypothesis, as it could explain distinct levels of endemism in different

372   portions of the MAF.

373

374   *Caparaó highlands as a hotspot of divergence*

375   The Caparaó is the highest mountain massif in the AF, reaching ca. 2900 m asl. Despite

376   its small area compared to the neighbouring highlands (Fig. 1), this mountain system not only

377   harbors a strongly differentiated population of *Microspingus* warbling-finches, but also

378   endemic taxa (*i.e. Caparaonia* lizards, Rodrigues et al. 2009) whose divergences from taxa in

379   other larger AF highlands are possibly much older than our divergence estimates. This suggests

380   that the Caparó highlands possibly represent a microrefugium (*sensu* Rull 2009) with a

381   long-term history of connection and isolation with the neighboring highlands. This makes the

382   Caparaó highlands an overlooked hotspot of population divergence and cryptic diversity,

383   similarly to the Chapada Diamantina highlands (Amaral et al. 2013) and the Araripe plateau

384   (Amaral et al. 2018). The presence of both recent and old endemic lineages in the Caparaó

385   mountains may be related to higher population persistence in contrast to lower neighboring

386   mountains. Interestingly, although the Caparáo population of *M. lateralis* diverged from the

387   remaining *M. lateralis* populations, genetic differentiation was not detected between the other

388   two currently isolated (by the warm lowlands of the Paraíba do Sul river valley) Serra do Mar

389   and Serra da Mantiqueira populations. This could be related to a greater geographic proximity

390   between the latter, thus allowing genetic homogeinization. Given that population size changes

391   may be buffered by shifts in elevational ranges and that extreme interglacial-warm periods

392   could crash mountain-top populations (Moritz et al. 2008), it is possible that higher mountain

393   ranges are related to higher persistence, higher levels of endemicity, wider temporal ranges of

394   population divergence compared to lower neighboring mountain ranges. Populations of many

395   species that occur in Mantiqueira and Serra do Mar mountain systems can also be found in

396   Caparaó and offer exciting future opportunities to identify cryptic diversity.

397

398   *The São Paulo and Caparaó subtropical gaps*

399   Low passes and inter-mountain valleys often constitute formidable barriers to dispersal

400 in montane tropical organisms (e.g. Africa - Bowie et al. 2006; Andes - Cadena et al. 2007,

401 Winger and Bates 2015). However, such ecological barriers to genetic exchange remain largely

402 overlooked in the MAF biota. In our study, more than 100 kilometers of lowlands that reach

403 elevations down to 250 m a.s.l. in the Ribeira de Iguape River Valley (Karl et al. 2013) separate

404 *M. lateralis* from *M. cabanisi*. This coincides with range and phenotypic discontinuities in

405 other cold-adapted avian species complexes, including passerines (e.g. *Hemitriccus* flycatchers,

406 *C. thoracica* warbling-finch) and non-passerines (*Stephanoxis* hummingbirds, Cavarzere et al.

407 2014), as well as with a narrow zone of secondary contact between cold-adapted lineages of

408 *Bombus* bees (Françoso et al. 2016). Lower elevation forests also seem to isolate the highland

409 biota of Caparaó from the ones of southern mountain ranges. We suggest that these lower

410 elevation forests represent the ecological barrier underlying the differentiation in these and

411 possibly other MAF organisms and could be named "São Paulo subtropical gap" and "Caparaó

412 subtropical gap". These ecological gaps highlights the influence of historical climate changes

413 and associated shifts in the geographic distribution of MAF organisms, and coincides with the

414 genetic differentiation observed in our study system. Additional studies will show if the

415 historical processes affecting montane organisms in this region are shared, thus generating

416 population divergence in other co-distributed organisms.

417

Literature cited

438
439   Akaike H (1973) Information theory and an extensión of the maximum likelihood principle.
440   *International symposium on information theory*, 267–281.

441   Almeida FFM, Carneiro CDR (1998) Origem e evloução da Serra do Mar. *Revista Brasileira*
442   *de Geociências*, **28**, 135–150.

443   Amaral FR, Piacentini VQ, Brito GRR, Curcio FF (2012) A simple and effective air shotgun
444   for collecting small birds and other vertebrates at close range. *Journal of Field*
445   *Ornithology*, **83**, 403–406.

446   Amaral FR, Neves LG, Resende Jr MFR *et al.* (2015) Ultraconserved Elements Sequencing as
447   a Low-Cost Source of Complete Mitochondrial Genomes and Microsatellite Markers in
448   Non-Model Amniotes. *PLoS ONE*, **10**, e0138446.

449   Amaral FR, Albers PK, Edwards S V, Miyaki CY (2013) Multilocus tests of Pleistocene
450   refugia and ancient divergence in a pair of Atlantic Forest antbirds (Myrmeciza).
451   *Molecular Ecology*, **22**, 3996–4013.

452   Amaral FR, Maldonado-Coelho M, Aleixo A, Luna LW, Rêgo PS, Araripe J, Souza TO, Thom,
453   G. 2018. Recent chapters of Neotropical history overlooked in phylogeography: Shallow
454   divergence explains phenotype and genotype uncoupling in Antilophia manakins.
455   *Molecular Ecology.*

456   Amaro RC, Rodrigues MT, Yonenaga-Yassuda Y, Carnaval AC (2012) Demographic
457   processes in the montane Atlantic rainforest: Molecular and cytogenetic evidence from the
458   endemic frog *Proceratophrys boiei*. *Molecular Phylogenetics and Evolution*, **62**,
459   880–888.

460   Andrews S (2014) FastQC: A quality control tool for high throughput sequence data.
461   http://www.bioinformatics.babraham.ac.uk/projects/fastqc/.

462   Antonelli A (2015) Biodiversity: Multiple origins of mountain life. *Nature*, **524,** 300-301.

463   Assis CP, Raposo MA, Parrini R (2007) Validação de Poospiza cabanisi Bonaparte, 1850

464 (Passeriformes: Emberizidae). *Revista Brasileira de Ornitologia*, 15, 103–112.

465 Badgley C (2010) Tectonics, topography, and mammalian diversity. *Ecography*, **33**, 220–231.

466 Barry, R. G. (1992). Mountain weather and climate (Third edition). Cambridge University
467 Press.

468 Batalha-Filho H, Cabanne GS, Miaki CY (2012) Phylogeography of an Atlantic Forest
469 passerine reveals demographic stability through the last glacial maximum. *Molecular*
470 *Phylogenetics and Evolution*, **65**, 892–902.

471 Behling H (1997) Late Quaternary vegetation, climate and fire history from the tropical
472 mountain region of Morro de Itapeva, SE Brazil. *Palaeogeography, Palaeoclimatology,*
473 *Palaeoecology,* **129**, 407–422.

474 Behling H (2007) Late Quaternary vegetation, fire and climate dynamics of Serra do Araçatuba
475 in the Atlantic coastal mountains of Paraná State, southern Brazil. *Vegetation History and*
476 *Archaeobotany*, **16**, 77–85

477 Behling H, Pillar V (2007) Late Quaternary vegetation, biodiversity and fire dynamics on the
478 southern Brazilian highland and their implication for conservation and management of
479 modern Araucaria forest and grassland ecosystems. *Philosophical Transactions of the*
480 *Royal Society of London Series B Biological Sciences*, **362**, 243–251.

481 Behling H, Dupont L, Safford HD, Wefer, G (2007) Late Quaternary vegetation and climate
482 dynamics in the Serra da Bocaina, southeastern Brazil. *Quaternary International*, **161**,
483 22–31.

484 Behling H, Safford, HD (2010) Late-glacial and Holocene vegetation, climate and fire
485 dynamics in the Serra dos Orgãos Mountains of Rio de Janeiro State, southeastern Brazil.
486 *Global Change Biology*, **16**, 1661–1671.

487 Bolger AM, Lohse M, Usadel B (2014) Trimmomatic: a flexible trimmer for Illumina
488 sequence data. *Bioinformatics*, **30**, 2114-2120.

489 Bowie RCK, Fjeldså J, Hackett SJ, Bates JM, Crowe TM (2006) Coalescent models reveal the
490 relative roles of ancestral polymorphism, vicariance, and dispersal in shaping
491 phylogeographical structure of an African montane forest robin. *Molecular Phylogenetics*
492 *and Evolution*, **38,** 171–188.

493 Brown JH (1971) Mammals on Mountaintops: Nonequilibrium Insular Biogeography. *The*
494 *American Naturalist*, **105**, 467.

495 Brown Jr., K. S., & Ab'Saber, A. N. (1979). Ice-age forest refuges and evolution in the
496 neotropics: correlation of paleoclimatological, geomorphological and pedological data
497 with modern biological endemism. *Paleoclimas*, **5**, 1–30.

498 Brown KSJr (1987) Conclusions, synthesis and alternative hypotheses. In: Whitmore, T. C.
499   and G. T. Prance (eds). Biogeography and Quaternary History in Tropical America.
500   Oxford Science Publications.
501 Cabanne GS, Santos FS, Miyaki CY (2007) Phylogeography of *Xiphorhynchus fuscus*
502   (Passeriformes, Dendrocolaptidae): vicariance and recent demographic expansion in
503   southern Atlantic forest. *Biological Journal of the Linnean Society*, **91**, 73–84.
504 Cadena CD, Klicka J, Ricklefs RE (2007) Evolutionary differentiation in the Neotropical
505   montane region: molecular phylogenetics and phylogeography of *Buarremon*
506   brush-finches (Aves, Emberizidae). *Molecular Phylogenetics and Evolution*, **44**,
507   993–1016.
508 Carnaval AC, Hickerson MJ, Haddad CFB, Rodrigues MT, Moritz C (2009) Stability predicts
509   genetic diversity in the Brazilian Atlantic Forest hotspot. *Science*, **323**, 785–789.
510 Carnaval AC, Waltari E, Rodrigues MT, Rosauer D, VanDerWal J, Damasceno R, Prates I,
511   Strangas M, Spanos Z, Rivera D, Pie MR, Firkowski CR, Bornschein MR, Ribeiro LF,
512   Moritz C (2014). Prediction of phylogeographic endemism in an environmentally
513   complex biome. Proceedings of the Royal Society B: Biological Sciences, **281,** 20141461.
514 Cavarzere, V., Silveira, L. F., Vasconcelos, M. F. de, Grantsau, R., & Straube, F. C. (2014).
515   Taxonomy and biogeography of *Stephanoxis* Simon, 1897 (Aves: Trochilidae). *Papéis*
516   *Avulsos de Zoologia*, **54,** 69-79.
517 Chen IC, Shiu HJ, Benedick S, Holloway JD, Chey VK, Barlow HS, Hill JK, Thomas CD
518   (2009) Elevation increases in moth assemblages over 42 years on a tropical mountain.
519   *Proceedings of the National Academy of Sciences of the United States of America*, **106**,
520   1479–1483.
521 Cogné N, Gallagher K, Cobbold PR, Riccomini C, Gautheron C (2012) Post-breakup tectonics
522   in southeast Brazil from thermochronological data and combined inverse-forward thermal
523   history modeling. *Journal of Geophysical Reserach*, **117**, B11413.
524   Excoffier L, Dupanloup I, Huerta-Sánchez E, Sousa VC, Foll M (2013) Robust
525   Demographic Inference from Genomic and SNP Data. *PLoS Genetics*, **9**.
526 Faircloth BC, McCormack JE, Crawford NG, Harvey MG, Brumfield RT, Glenn TC (2012)
527   Ultraconserved elements anchor thousands of genetic markers spanning multiple
528   evolutionary timescales. *Systematic Biology*, 61, 717–726.
529 Faircloth BC (2014) Illumiprocessor: a Trimmomatic wrapper for parallel adapter and quality
530   trimming. https://github.com/faircloth-lab/illumiprocessor.
531 Faircloth BC (2014) Phyluce: phylogenetic estimation from ultraconserved elements.

532   https://github.com/faircloth-lab/phyluce.

533 Fjeldså, J. (1994). Geographical patterns for relict and young species of birds in Africa and

534   South America and implications for conservation priorities. *Biodiversity & Conservation*,

535   **3**, 207–226.

536 Fjeldså J, Lambin E, Mertens B (1999). Correlation between Endemism and Local Ecoclimatic

537   Stability Documented by Comparing Andean Bird Distributions and Remotely Sensed

538   Land Surface Data. Ecography, **22**, 63–78.

539 Fjeldså J, Bowie RCK, Rahbek C (2012). The Role of Mountain Ranges in the Diversification

540   of Birds. *Annual Review of Ecology, Evolution, and Systematics*. **43**, 249-265.

541 Franco‐Magalhaes AOB, Cuglieri MAA, Hackspacher PC, Saad AR (2014) Long‐term

542   landscape evolution and post‐rift reactivation in the southeastern Brazilian passive

543   continental margin: Taubaté basin. *International Journal of Earth Science*, **103**, 441–453.

544 Françoso E, Zuntini AR, Carnaval AC, Arias MC (2016). Comparative phylogeography in the

545   Atlantic forest and Brazilian savannas: pleistocene fluctuations and dispersal shape spatial

546   patterns in two bumblebees. BMC Evolutionary Biology, 16(1), 267.

547 Freitas, RO (1951) Relevos policíclicos na tectônica do escudo Brasileiro. *Boletim Paulista*

548   *Geociências*, **7**, 3–19.

549 Frichot E, Mathieu F, Trouillon T, Bouchard G, François O (2014) Fast and efficient

550   estimation of individual ancestry coefficients. *Genetics*, **196**, 973–983.

551 Frichot, E., & François, O. (2015). LEA: An R package for landscape and ecological

552   association studies. *Methods in Ecology and Evolution*, **6**, 925–929.

553 Firkowski CR, Bornschein MR, Ribeiro LF, Pie MR (2016). Species delimitation, phylogeny

554   and evolutionary demography of co-distributed, montane frogs in the southern Brazilian

555   Atlantic Forest. *Molecular Phylogenetics and Evolution*, **100**, 345–360.

556 Fjeldså J, Lambin E, Mertens B (1999). Correlation between Endemism and Local Ecoclimatic

557   Stability Documented by Comparing Andean Bird Distributions and Remotely Sensed

558   Land Surface Data. *Ecography*, **22**, 63–78.

559 Graham CH, Carnaval AC, Cadena CD, Zamudio KR, Roberts TE, Parra JL, McCain CM,

560   Bowie RC, Moritz C, Baines SB, Schneider CJ, VanDerWal J, Rahbek C, Kozak KH,

561   Sanders NJ (2014) The origin and maintenance of montane diversity: Integrating

562   evolutionary and ecological processes. *Ecography*, **37**, 711–719.

563   Gutenkunst RN, Hernandez RD, Williamson S H, Bustamante CD (2009). Inferring the

564   Joint Demographic History of Multiple Populations from Multidimensional SNP

565   Frequency Data. PLOS Genetics, 5(10), e1000695.

566   Hackspacher PC, Ribeiro LFB, Ribeiro MCS, Fetter AH, Hadler Neto JC, Tello Saenz CA,

567   Dantas EL (2004) Consolidation and break-up of the South American platform in

568   Southeastern Brazil: tectonothermal and denudation histories. *Gondwana Research*, **7**,

569   91–101.

570 Hooghiemstra H, Van der Hammen T (2004) Quaternary ice-age dynamics in the Colombian

571   Andes: developing an understanding of our legacy. *Philosophical Transactions of the*

572   *Royal Society B: Biological Sciences*, **359**, 173–181.

573 Karl M, Glasmacher UA, Kollenz S, Franco-Magalhaes AOE, Stockli DF, Hackspacher PC

574   (2013) Evolution of the South Atlantic passive continental margin in southern Brazil

575   derived from zircon and apatite (U–Th–Sm)/He and fission-track data. *Tectonophysics*,

576   **604**, 224–244.

577 Knowles LL, Massatti R. (2016). Distributional shifts – not geographic isolation – as a

578   probable driver of montane species divergence. *Ecography*, **40**, 1475–1485.

579 Jombart T, Devillard S, Balloux F (2010) Discriminant analysis of principal components: a

580   new method for the analysis of genetically structured populations. *BMC genetics*, **11**, 94.

581   Ledru M-P, Mourguiart P, Riccomini C (2009) Related changes in biodiversity, insolation

582   and climate in the Atlantic rainforest since the last interglacial. *Palaeogeography,*

583   *Palaeoclimatology, Palaeoecology*, **271**, 140–152

584 Leigh JW, Bryant D. (2015). popart: full-feature software for haplotype network construction.

585   *Methods in Ecology and Evolution*, **6**, 1110–1116.

586   Li H (2013) Aligning sequence reads, clone sequences and assembly contigs with

587   BWA-MEM. *arXiv preprint arXiv:1303.3997*.

588 Mastretta-Yanes A, Xue AT, Moreno-Letelier A, Jorgensen TH, Alvarez N, Piñero D,

589   Emerson BC (2018). Long-term in situ persistence of biodiversity in tropical sky islands

590   revealed by landscape genomics. *Molecular Ecology*, **27**, 432–448.

591 Maldonado-Coelho M (2012) Climatic oscillations shape the phylogeographical structure of

592   Atlantic Forest fire-eye antbirds (Aves: Thamnophilidae). *Biological Journal of the*

593   *Linnean Society*, **105**, 900–924.

594 Mayr E, Diamond JM (1976) Birds on islands in the sky: Origin of the montane avifauna of

595   Northern Melanesia. *Proceedings of the National Academy of Sciences of the United*

596   *States of America*, **73**, 1765–1769.

597 McCormack JE, Huang H, Knowles LL (2009) Sky islands. *Encyclopedia of Islands*, **4**,

598   841–843.

599   McKenna A, Hanna M, Banks E, Sivachenko A, Cibulskis K, Kernytsky A, Garimella K,
600   Altshuler D, Gabriel S, Daly M, DePristo MA (2010) The genome analysis toolkit: A
601   MapReduce framework for analyzing next-generation DNA sequencing data. *Genome*
602   *Research*, **20**, 1297–1303.

603   Meisling KE, Cobbold PR, Mount VS (2001) Segmentation of an obliquely rifted margin,
604   Campos and Santos basins, southeastern Brazil. *AAPG Bulletin*, **85**, 1903–1924.

605   Melo MS, Riccomini C, Hasui Y, Almeida FFMA, Coimbra AM (1985) Geologia e evolução
606   do sistema de bacias tafrogênicas continentais do sudeste do Brasil. *Revista Brasileira de*
607   *Geociências*, **15**, 193–201.

608   Modenesi-Gauttieri MC, Hiruma ST, Riccomini C (2002) Morphotectonics of a high plateau
609   on the northwestern flank of the Continental Rift of southeastern Brazil *Geomorphology*,
610   **43**, 257–271.

611   Moritz C, Patton JL, Conroy CJ, Parra JL, White GC, Beissinger SR (2008) Impact of a century
612   of climate change on small-mammal communities in Yosemite National Park, USA.
613   *Science (New York, N.Y.)*, **322**, 261–264.

614   Nadachowska-Brzyska K, Li C, Smeds L, Zhang G, Ellegren H (2015). Temporal Dynamics of
615   Avian Populations during Pleistocene Revealed by Whole-Genome Sequences. *Current*
616   *Biology*, **25**, 1375–1380.

617   Oliveira MAT, Behling H, Pessenda LCR (2008) Late-Pleistocene and midHolocene
618   environmental changes in highland valley head areas of Santa Catarina State, Southern
619   Brazil. *Journal of South American Earth Sciences*, **26**, 55-67.

620   Oliveira MAT, Porsani JL, Lima GL, Jeske-Pieruschka V, Behling H (2012) Late Pleistocene
621   to Holocene peatland evolution in southern Brazilian highlands as depicted by radar
622   stratigrahy, sedimentology and palynology. *Quaternary Research*, **77**, 397-407.

623   Patton JL, Smith MF (1992) mtDNA phylogeny of Andean mice: a test of diversification
624   across ecological gradients. Evolution **46**, 174–183.

625   Peres EA, Sobral-Souza T, Perez MF, Bonatelli IA, Silva DP, Silva MJ, Solferini VN (2015)
626   Pleistocene niche stability and lineage diversification in the subtropical spider Araneus
627   omnicolor (Araneidae). *PloS one*, **10**, e0121543.

628   Pie MR, Faircloth BC, Ribeiro LF, Bornschein MR, Mccormack JE (2018). Phylogenomics of
629   montane frogs of the Brazilian Atlantic Forest is consistent with isolation in sky islands
630   followed by climatic stability. Biological Journal of the Linnean Society, 125, 72–82.

631   Rodrigues MT, Cassimiro J, Pavan D, Curcio FF, Verdade VK, Pellegrino KCM (2009). A
632   New Genus of Microteiid Lizard from the Caparaó Mountains, Southeastern Brazil, with a

Discussion of Relationships among Gymnophthalminae (Squamata). *American Museum Novitates*, **3673,** 1–27.

Stotz, D. F., Fitzpatrick, J. W., Parker III, T. A., & Moskovits, D. K. (1996). Neotropical birds: ecology and conservation. University of Chicago Press.

Tello Saenz CA, Hackspacher PC, Hadler Neto JC, Iunes PJ, Guedes S, Paulo SR, Ribeiro LFB (2003) Recognition of cretaceous, paleocene and neogene tectonic reactivation, through apatite fission-track analysis, in Precambrian areas of the Southeast Brazil: association with the South Atlantic Ocean opening. *Journal of South American Earth Science*, **15**, 137–142.

Thomé MTC, Zamudio KR, Haddad CFB, Alexandrino J (2014) Barriers, rather than refugia, underlie the origin of diversity in toads endemic to the Brazilian Atlantic Forest. *Molecular Ecology*, **23**, 6152–6164.

Thomé MT, Zamudio KR, Giovanelli JG, Haddad CF, Baldissera FA Jr, Alexandrino J (2010) Phylogeography of endemic toads and post-Pliocene persistence of the Brazilian Atlantic Forest. *Molecular Phylogenetics and Evolution*, **55**, 1018–1031.

Winger BM, Bates JM (2015) The tempo of trait divergence in geographic isolation: avian speciation across the Marañon valley of Peru. *Evolution*, **69**, 772–782.

Zamudio KR, Bell RC, Mason NA (2016). Phenotypes in phylogeography: Species' traits, environmental variation, and vertebrate diversification. *Proceedings of the National Academy of Sciences of the United States of America*, **113**, 8041–8048.

666 **Figures and tables**

667

668 **Table 1.** Composite likelihood (Max ln(L)), number of parameter (param), Akaike

669 information criterion (AIC) and relative contribution (Weights) for each of the demographic

670 models tested. The name of the models represent the topology, in newick format and the

671 demographic syndromes tested (see Figure 3). mc - *Microspingus cabanisi*; ml - *Microspingus*

672 *lateralis*; cp - Caparaó population of *Microspingus lateralis.* In bold: best model.

673

Model	Max ln(L)	param	AIC	Weights
(cp(mc,ml)_no_gene_flow	-984,043	7	4545,69	7,59E-14
(mc(ml,cp)_no_gene_flow	-992,599	7	4585,09	2,11E-22
(ml(mc,cp)_no_gene_flow	-995,667	7	4599,22	1,80E-25
polytomy_no_gene_flow	-995,458	5	4594,25	2,16E-24
(cp(mc,ml)_gene_flow	-969,639	13	4491,35	4,77E-02
(ml(mc,cp)_gene_flow	-969,7	13	4491,63	4,15E-02
(mc(ml,cp)_gene_flow	-969,165	13	4489,17	1,42E-01
polytomy_gene_flow	**-969,301**	**11**	**4485,80**	**7,68E-01**
(cp(mc,ml)_bottleneck_gene_flow	-969,658	19	4503,44	1,13E-04
(mc(ml,cp)_bottleneck_gene_flow	-971,675	19	4512,73	1,09E-06
(ml(mc,cp)_bottleneck_gene_flow	-968,982	19	4500,33	5,37E-04
polytomy_bottleneck_gene_flow	-970,391	17	4502,82	1,55E-04

674

675

676

677

678

679

680 **Table 2**. Parameter values of simulated models with the best likelihood in Fastsimcoal2. The

681 name of the models represent the topology, in newick format and the demographic syndromes

682 tested (see Figure 3). In bold: best model.

Model	Ne cp	Ne ml	Ne mc	Ne a1	Ne a2	NMcp/ml	NMml/cp	NMcp/mc	NMmc/cp	NMml/mc
(cp(mc,ml))_no_gene_flow	7862	17744	36326	54255	1610	n/a	n/a	n/a	n/a	n/a
(mc(ml,cp))_no_gene_flow	5249	32714	75535	185893	5687	n/a	n/a	n/a	n/a	n/a
(ml(mc,cp))_no_gene_flow	4485	23123	44924	9689	7660	n/a	n/a	n/a	n/a	n/a
polytomy_no_gene_flow	4125	17300	33859	n/a	9138	n/a	n/a	n/a	n/a	n/a
(cp(mc,ml))_gene_flow	7562	20728	38539	8463	6663	0,36	1,70	0,67	0,01	2,35
(ml(mc,cp))_gene_flow	7254	23247	47682	6049	7555	0,52	1,44	0,08	0,62	3,70
(mc(ml,cp))_gene_flow	9519	40571	61488	11273	5941	0,21	1,68	0,15	0,47	3,98
polytomy_gene_flow	**3866**	**10944**	**18842**	**n/a**	**4552**	**0,32**	**1,15**	**0,49**	**0,98**	**3,15**
(cp(mc,ml))_bottleneck_gene_flow	8065	22007	51902	8229	2018	0,48	1,06	0,38	0,48	3,01
(mc(ml,cp))_bottleneck_gene_flow	7305	22418	41563	4746	2553	0,48	0,18	0,45	0,52	3,43
(ml(mc,cp))_bottleneck_gene_flow	6053	18163	41631	6229	5336	0,38	0,63	0,43	0,01	2,74
polytomy_bottleneck_gene_flow	4161	14562	30245	n/a	3160	0,41	0,02	0,35	0,01	3,78
polytomy_gene_flow lo 95% CI	**1243**	**7319**	**20345**	**n/a**	**7839**	**0,19**	**0,02**	**0,22**	**0,00**	**1,77**
polytomy_gene_flow up 95% CI	**4337**	**19877**	**40176**	**n/a**	**41635**	**0,78**	**0,84**	**1,55**	**0,56**	**2,95**

Model	NMmc/ml	TDIV1	TDIV2	SCcp	SCml	SCmc	TSCcp	TSCml	TSCmc
(cp(mc,ml)_no_gene_flow	n/a	3159	8984	n/a	n/a	n/a	n/a	n/a	n/a
(mc(ml,cp)_no_gene_flow	n/a	4926	10049	n/a	n/a	n/a	n/a	n/a	n/a
(ml(mc,cp)_no_gene_flow	n/a	5082	5415	n/a	n/a	n/a	n/a	n/a	n/a
polytomy_no_gene_flow	n/a	n/a	4380	n/a	n/a	n/a	n/a	n/a	n/a
(cp(mc,ml)_gene_flow	3,20	9637	15832	n/a	n/a	n/a	n/a	n/a	n/a
(ml(mc,cp)_gene_flow	2,03	10448	16403	n/a	n/a	n/a	n/a	n/a	n/a
(mc(ml,cp)_gene_flow	1,97	17042	23414	n/a	n/a	n/a	n/a	n/a	n/a
polytomy_gene_flow	**2,65**	**n/a**	**8742**	**n/a**	**n/a**	**n/a**	**n/a**	**n/a**	**n/a**
(cp(mc,ml)_bottleneck_gene_flow	0,15	21967	35353	8,31	7,03	7,26	6068	7529	7524
(mc(ml,cp)_bottleneck_gene_flow	1,42	15331	16823	2,05	6,87	3,41	3499	3883	4519
(ml(mc,cp)_bottleneck_gene_flow	3,47	14064	15042	6,22	3,86	5,28	2583	2972	4031
polytomy_bottleneck_gene_flow	1,55	n/a	12407	38,15	5,53	19,06	1777	1602	1881
polytomy_gene_flow lo 95% CI	**0,68**	**n/a**	**10140**	**n/a**	**n/a**	**n/a**	**n/a**	**n/a**	**n/a**
polytomy_gene_flow up 95% CI	**4,25**	**n/a**	**47404**	**n/a**	**n/a**	**n/a**	**n/a**	**n/a**	**n/a**

683

684 mc - *Microspingus cabanisi*; ml - *Microspingus lateralis*; cp - Caparaó population of

685 *Microspingus lateralis.* Ne - effective population size; a1 - ancestral population after the first

686 divergence event backwards in time; a2 - ancestral population; NMx/y - number of migrants

687 per generation going from population x to y backwards in time; TDIV1 - first divergence event

688 backwards in time; TDIV2 second divergence event backwards in time; SC - proportion of the

689   ancestral effective population size in relation to the present, before instantaneous population

690   size change; TSC - Time of the instantaneous population size changes.
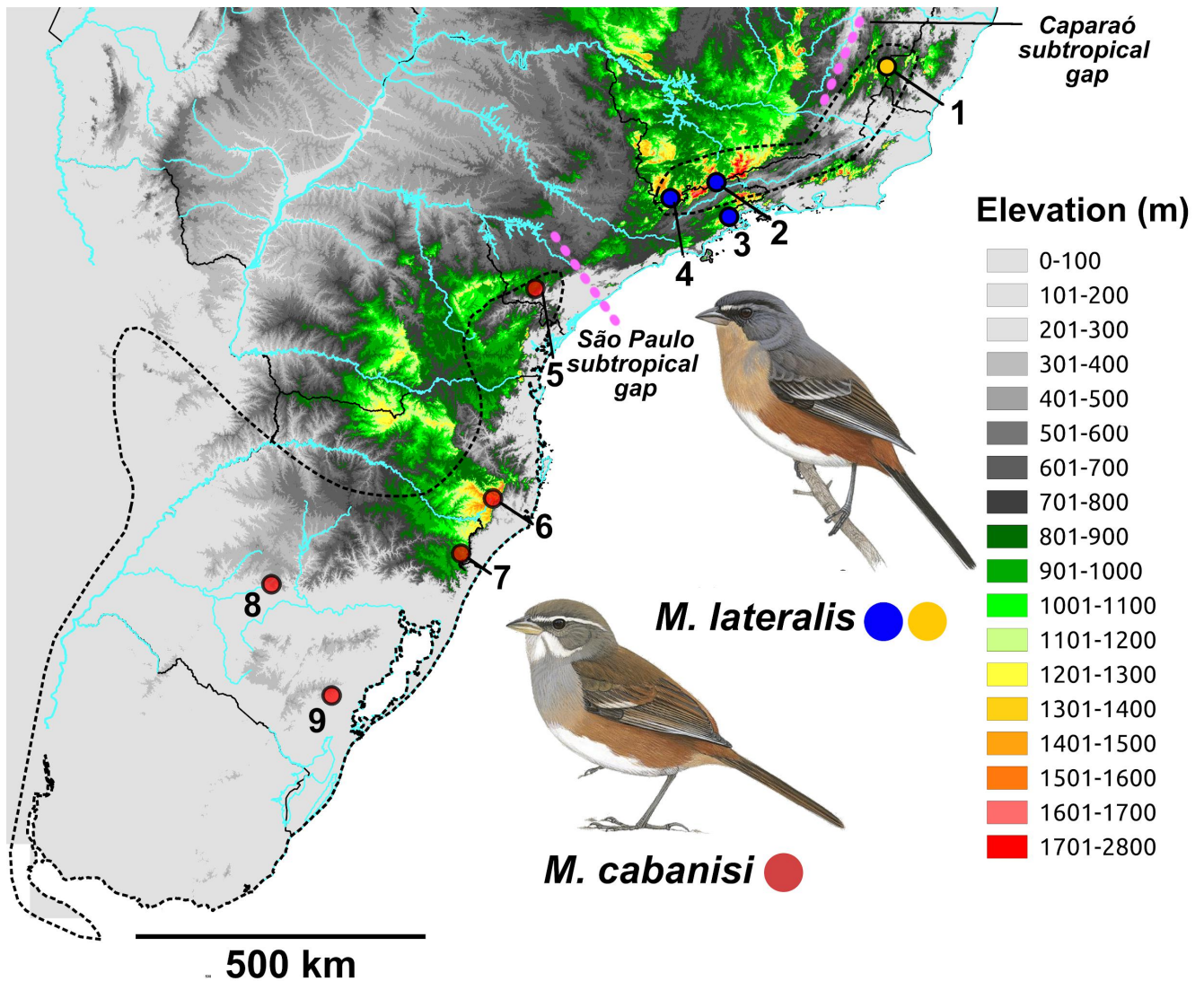
691

692

693

694

695

696

697

698

699

700

701

702

703

704
705
706

Figure 1. Localities sampled. Blue and yellow circles represent *Microspingus lateralis* while red circles represent *Microspingus cabanisi*. Major highlands include Caparaó (1), Northern Serra do Mar (2), Mantiqueira (3 and 4), Southern Serra do Mar (5) and Serra Geral (6 and 7). Two lower elevation regions that mark phenotypic and genotypic shifts, named here Caparaó and São Paulo subtropical gaps, are indicated by pink dashed lines. See Supplementary Information Table S1 for details on samples and coordinates.
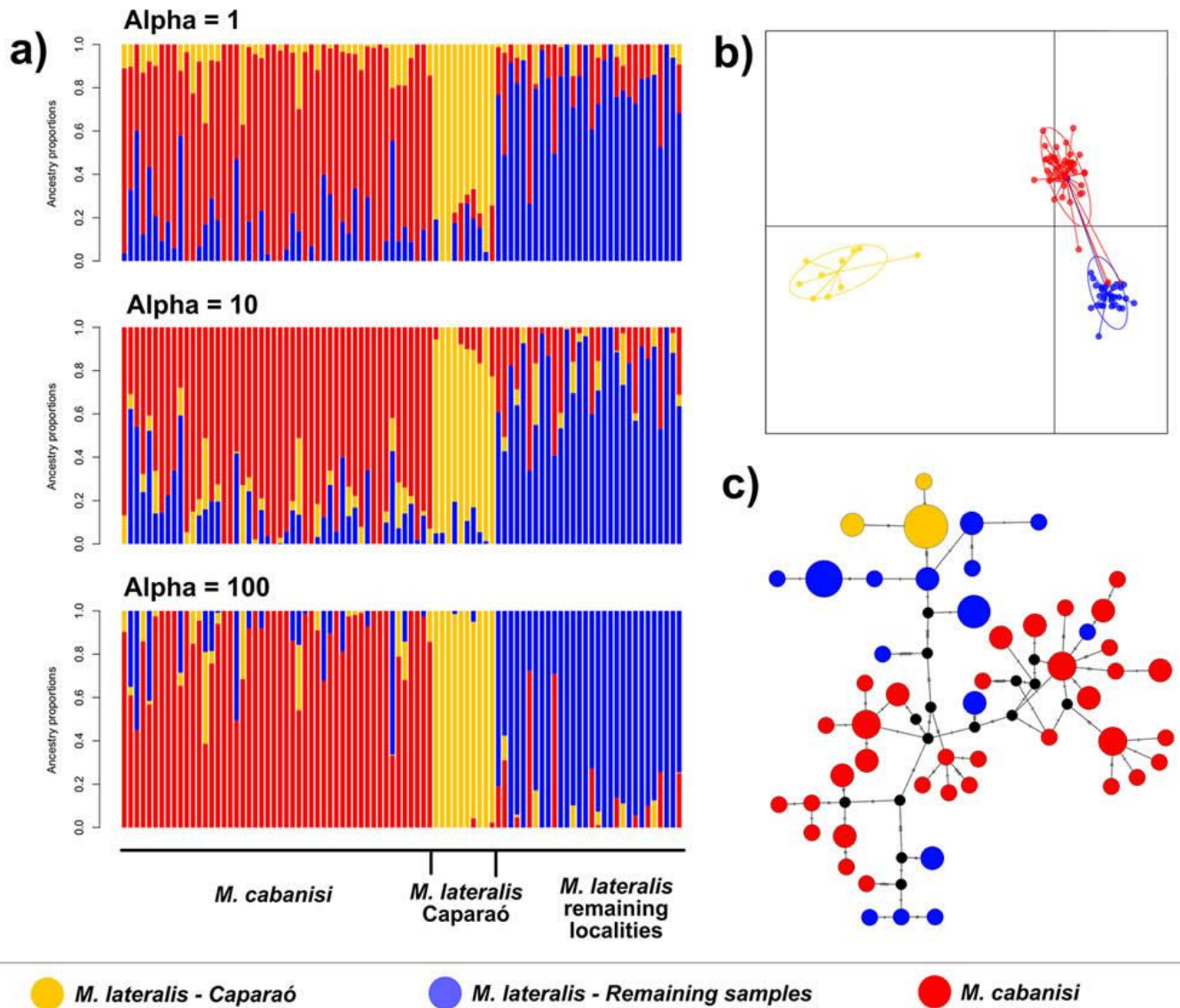
713
714
715
716
717

Figure 2. Plots depicting population structure according to (a) the best fitting sNMF model K=3 based on different values of the regularization parameter alpha (1, 10, 100) and (b) the three clusters inferred with DAPC and (c) cytochrome-b median-joining network. Black dots in the haplotype network indicate inferred haplotypes.
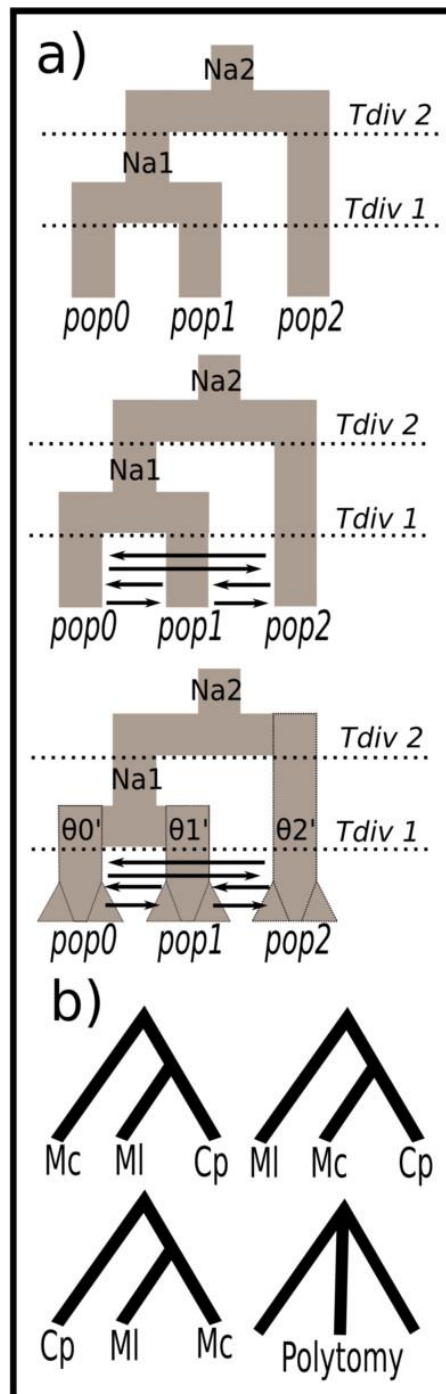
728

729

730 **Figure 3**. Demographic models simulated in Fastsimcoal2 for (a) three populations and (b)

731 alternative topologies tested under these demographic scenarios, in a total of 12 simulated

732 models. Na – ancestral effective population size; θ' – effective population size before

733 population size change; Tdiv – divergence time; Mc – *Microspingus cabanisi*; Ml –

734 *Microspingus lateralis*; Cp - Caparaó population of *Microspingus lateralis*

735

736 **Supplementary Information**

737 **Table S1**. Samples used in the present study.

738

739

Field number	Species	Locality number	Municipality	Latitude	Longitude	MZUSP number	LGEMA number
FRA46	*Poospiza lateralis*	1	Dores do Rio Preto	-20,5125	-41,8075	pending	pending
FRA49	*Poospiza lateralis*	1	Caparaó	-20,4097	-41,8376	pending	pending
FRA50	*Poospiza lateralis*	1	Caparaó	-20,4097	-41,8376	pending	pending
FRA52	*Poospiza lateralis*	1	Alto Jequitibá	-20,4074	-41,8382	pending	pending
FRA54	*Poospiza lateralis*	1	Caparaó	-20,4097	-41,8376	pending	pending
FRA55	*Poospiza lateralis*	1	Caparaó	-20,4748	-41,8291	pending	pending
FRA56	*Poospiza lateralis*	1	Espera Feliz	-20,4861	-41,8211	pending	pending
FRA57	*Poospiza lateralis*	1	Caparaó	-20,4792	-41,8297	pending	pending
FRA58	*Poospiza lateralis*	1	Caparaó	-20,4806	-41,8298	pending	pending
FRA59	*Poospiza lateralis*	1	Caparaó	-20,4722	-41,8267	pending	pending
MA02	*Poospiza lateralis*	2	Delfim Moreira	-22,5442	-45,2108	pending	pending
MA03	*Poospiza lateralis*	2	Delfim Moreira	-22,5444	-45,2073	pending	pending

MA04	*Poospiza lateralis*	2	Delfim Moreira	-22,5426	-45,1897	pending	pending
MA05	*Poospiza lateralis*	2	Delfim Moreira	-22,5429	-45,1837	pending	pending
FRA05	*Poospiza lateralis*	2	Delfim Moreira	-22,5446	-45,2158	pending	pending
FRA06	*Poospiza lateralis*	2	Piquete	-22,5160	-45,1521	pending	pending
FRA07	*Poospiza lateralis*	2	Piquete	-22,5696	-45,2276	pending	pending
FRA08	*Poospiza lateralis*	2	Piquete	-22,5159	-45,1510	pending	pending
FRA09	*Poospiza lateralis*	2	Piquete	-22,5693	-45,2291	pending	pending
FRA11	*Poospiza lateralis*	2	Piquete	-22,5160	-45,1507	pending	pending
FRA13	*Poospiza lateralis*	3	Cunha	-23,1438	-44,8761	pending	pending
FRA14	*Poospiza lateralis*	3	Paraty (PN Serra da Bocaina)	-23,1722	-44,8339	pending	pending
FRA16	*Poospiza lateralis*	3	Paraty (PN Serra da Bocaina)	-23,1673	-44,8396	pending	pending
FRA17	*Poospiza lateralis*	3	Paraty (PN Serra da Bocaina)	-23,1734	-44,8366	pending	pending
FRA19	*Poospiza lateralis*	3	Cunha	-23,1516	-44,8353	pending	pending
FRA20	*Poospiza lateralis*	3	Paraty (PN Serra da Bocaina)	-23,1516	-44,8215	pending	pending
FRA21	*Poospiza lateralis*	3	Cunha	-23,1526	-44,8417	pending	pending

FRA22	*Poospiza lateralis*	3	Cunha	-23,1491	-44,9328	pending	pending
FRA26	*Poospiza lateralis*	3	Cunha	-23,2053	-44,9966	pending	pending
FRA27	*Poospiza lateralis*	3	Cunha	-23,1386	-44,9064	pending	pending
MV01	*Poospiza lateralis*	4	Camanducaia	-22,8378	-46,0551	pending	pending
MV02	*Poospiza lateralis*	4	Camanducaia	-22,8584	-46,0664	pending	pending
MV03	*Poospiza lateralis*	4	Camanducaia	-22,8419	-46,0606	pending	pending
MV04	*Poospiza lateralis*	4	Camanducaia	-22,8419	-46,0606	pending	pending
MV05	*Poospiza lateralis*	4	Camanducaia	-22,8036	-46,0473	pending	pending
MV07	*Poospiza lateralis*	4	Camanducaia	-22,8214	-46,0438	pending	pending
FRA01	*Poospiza lateralis*	4	Camanducaia	-22,8499	-46,0642	pending	pending
FRA02	*Poospiza lateralis*	4	Camanducaia	-22,8037	-46,0472	pending	pending
FRA03	*Poospiza lateralis*	4	Camanducaia	-22,8112	-46,0425	pending	pending
FRA04	*Poospiza lateralis*	4	Camanducaia	-22,8500	-46,0642	pending	pending
FRA28	*Poospiza cabanisi*	5	Apiaí	-24,4284	-48,6742	pending	pending
FRA29	*Poospiza cabanisi*	5	Apiaí	-24,4284	-48,6742	pending	pending

FRA32	*Poospiza cabanisi*	5	Apiaí	-24,4762	-48,8972	pending	pending
FRA33	*Poospiza cabanisi*	5	Apiaí	-24,4762	-48,8972	pending	pending
FRA34	*Poospiza cabanisi*	5	Apiaí	-24,4762	-48,8972	pending	pending
FRA39	*Poospiza cabanisi*	5	Apiaí	-24,4284	-48,6742	pending	pending
FRA40	*Poospiza cabanisi*	5	Apiaí	-24,4284	-48,6742	pending	pending
FRA41	*Poospiza cabanisi*	5	Apiaí	-24,4284	-48,6742	pending	pending
FRA42	*Poospiza cabanisi*	5	Apiaí	-24,4284	-48,6742	pending	pending
FRA43	*Poospiza cabanisi*	5	Apiaí	-24,4284	-48,6742	pending	pending
SC01	*Poospiza cabanisi*	6	Urubici (PN São Joaquim)	-28,1419	-49,6353	pending	pending
SC02	*Poospiza cabanisi*	6	Urubici (PN São Joaquim)	-28,1419	-49,6353	pending	pending
SC03	*Poospiza cabanisi*	6	Urubici (PN São Joaquim)	-28,1419	-49,6353	pending	pending
SC05	*Poospiza cabanisi*	6	Urubici (PN São Joaquim)	-28,1449	-49,6324	pending	pending
SC08	*Poospiza cabanisi*	6	Urubici (PN São Joaquim)	-28,1116	-49,4968	pending	pending
SC09	*Poospiza cabanisi*	6	Urubici (PN São Joaquim)	-28,1116	-49,4968	pending	pending
SC10	*Poospiza cabanisi*	6	Urubici (PN São Joaquim)	-28,1116	-49,4968	pending	pending

SC11	*Poospiza cabanisi*	6	Urubici (PN São Joaquim)	-28,1116	-49,4968	pending	pending
SC14	*Poospiza cabanisi*	6	Urubici (PN São Joaquim)	-28,1116	-49,4968	pending	pending
SC15	*Poospiza cabanisi*	6	Urubici (PN São Joaquim)	-28,1116	-49,4968	pending	pending
SC17	*Poospiza cabanisi*	7	Cambará do Sul (PN Aparados da Serra)	-29,1746	-50,1148	pending	pending
SC18	*Poospiza cabanisi*	7	Cambará do Sul (PN Aparados da Serra)	-29,1746	-50,1148	pending	pending
SC19	*Poospiza cabanisi*	7	Cambará do Sul (PN Aparados da Serra)	-29,1746	-50,1148	pending	pending
SC20	*Poospiza cabanisi*	7	Cambará do Sul (PN Aparados da Serra)	-29,1746	-50,1148	pending	pending
SC21	*Poospiza cabanisi*	7	Cambará do Sul (PN Aparados da Serra)	-29,1746	-50,1148	pending	pending
SC22	*Poospiza cabanisi*	7	Cambará do Sul (PN Aparados da Serra)	-29,1746	-50,1148	pending	pending
SC23	*Poospiza cabanisi*	7	Cambará do Sul (PN Aparados da Serra)	-29,1746	-50,1148	pending	pending
SC24	*Poospiza cabanisi*	7	Cambará do Sul	-29,1149	-50,1064	pending	pending
SC25	*Poospiza cabanisi*	7	Cambará do Sul (PN Serra Geral)	-29,1447	-50,0804	pending	pending
SC26	*Poospiza cabanisi*	7	Cambará do Sul	-29,0568	-50,1187	pending	pending
FRA74	*Poospiza cabanisi*	8	Itaara	-29,6130	-53,7529	pending	pending
FRA75	*Poospiza cabanisi*	8	Santa Maria	-29,5974	-53,7006	pending	pending

FRA76	*Poospiza cabanisi*	8	Santa Maria	-29,5974	-53,7006	pending	pending
FRA77	*Poospiza cabanisi*	8	Itaara	-29,5896	-53,7934	pending	pending
FRA78	*Poospiza cabanisi*	8	Itaara	-29,5920	-53,7521	pending	pending
FRA80	*Poospiza cabanisi*	8	Itaara	-29,5892	-53,7933	pending	pending
FRA81	*Poospiza cabanisi*	8	Itaara	-29,5929	-53,7598	pending	pending
FRA82	*Poospiza cabanisi*	8	Itaara	-29,5929	-53,7598	pending	pending
FRA84	*Poospiza cabanisi*	8	Itaara	-29,5937	-53,7343	pending	pending
FRA85	*Poospiza cabanisi*	8	Itaara	-29,5819	-53,8062	pending	pending
FRA61	*Poospiza cabanisi*	9	Pelotas	-31,6277	-52,5227	pending	pending
FRA62	*Poospiza cabanisi*	9	Pelotas	-31,6088	-52,5188	pending	pending
FRA64	*Poospiza cabanisi*	9	Pelotas	-31,6317	-52,5416	pending	pending
FRA65	*Poospiza cabanisi*	9	Pelotas	-31,6071	-52,5486	pending	pending
FRA66	*Poospiza cabanisi*	9	Pelotas	-31,6071	-52,5486	pending	pending
FRA67	*Poospiza cabanisi*	9	Pelotas	-31,5265	-52,5505	pending	pending
FRA68	*Poospiza cabanisi*	9	Pelotas	-31,5265	-52,5505	pending	pending

FRA69	*Poospiza cabanisi*	9	Pelotas	-31,5178	-52,5042	pending	pending
FRA71	*Poospiza cabanisi*	9	Canguçu	-31,4565	-52,6348	pending	pending
FRA72	*Poospiza cabanisi*	9	Canguçu	-31,4579	-52,6150	pending	pending

740

741

742

743

744

745

746

747

748

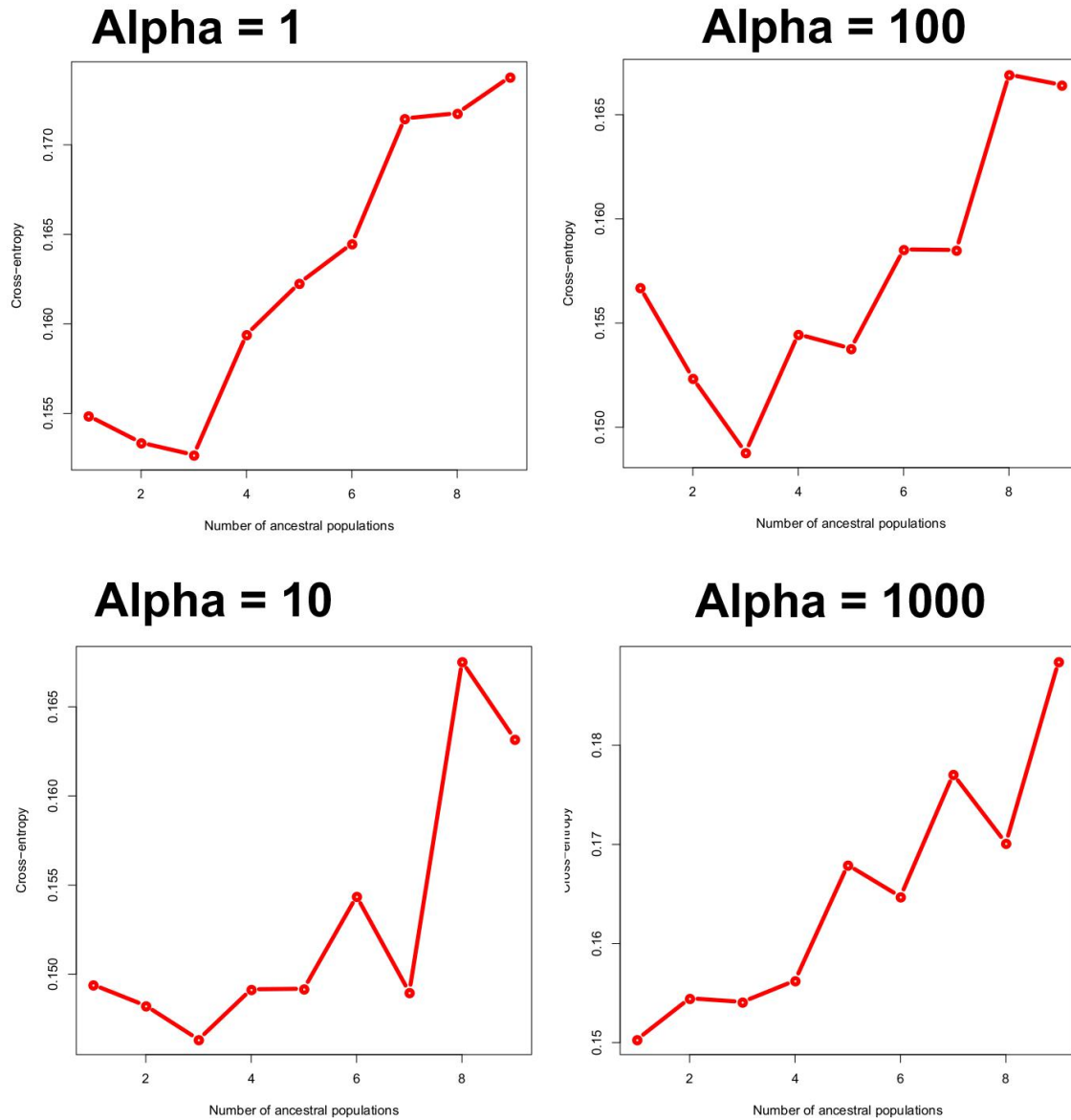749

750

751

752

753

754

755

756

757
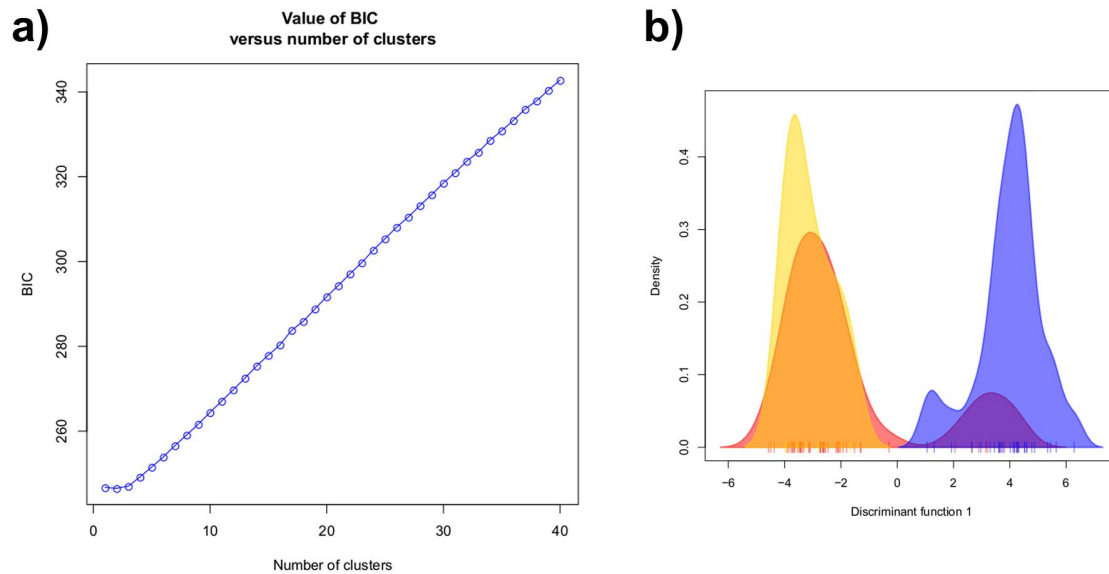
758

759

760

761

762

763

764

765

766

767

768

769 **Figure S1**. Cross-entropy sNMF runs for alpha values of 1, 10, 100 and 1,000.

770

771

772

a)

Value of BIC
versus number of clusters

b)

773

774 **Figure S2**. BIC values of (a) K-clustering method and (b) DAPC plot for two populations.

775 Colors in the DAPC plot follow the ones assumed for Figures 1 and 2.

776 **Data Accessibility**

777 Dryad XXXX and SRA XXXX

778

779 Raw Illumina files, Set of SNPs, Joint SFS

780

781 **Author contributions**

782

783 FRA, DFA and GT designed the study. FRA, JACM and GT performed field work. FRA,

784 DFAS and GT performed data analysis. FRA, KCMP, CYM and MJH contributed funds for lab

785 or field work. All authors participated in the discussion of the results. FRA, MMC and GT

786 wrote the manuscript with input from the other authors. All authors approved the final version

787 of the manuscript.